

Estimation of Kerr Nonlinearity in an Anti-resonant Hollow-Core Fiber by High-order QAM Transmission

Dawei Ge¹, Shoufei Gao², Mingqing Zuo¹, Yuyang Gao³, Yingying Wang², Baoluo Yan⁴, Bing Ye⁴, Dechao Zhang¹, Wei Ding^{2,*}, Han Li^{1,*}, and Zhangyuan Chen³

¹Department of Fundamental Network Technology, China Mobile Research Institute, Beijing 100053, China

²Institute of Photonics Technology, Jinan University, Guangzhou 510632, China

³State Key Laboratory of Advanced Optical Communication Systems and Networks, Peking University, Beijing 100871, China

⁴ZTE Corporation, Hebei 065201, China

*lihan@chinamobile.com, dingwei@jnu.edu.cn

Abstract: We propose a novel technique to measure Kerr nonlinearity in a hollow-core fiber based on nonlinear phase shift estimation by high-order QAM transmission. The measured $n_{2,\text{Kerr}}$ of the NANF-5 medium is $<2.20 \times 10^{-23} \text{ m}^2/\text{W}$. © 2023 The Author(s)

1. Introduction

Recent Anti-Resonant Hollow-Core Fiber (ARF) prototypes have shown a steady progress in loss properties [1-4] and widespread impacts in diverse optical communication scenarios including ultra-long-haul WDM systems [5], short-reach wide-band interconnects [6], classical channel coexistence with quantum key distribution [7], etc. For the purpose of predicting ultimate performances of data transmission through such novel fibers, accurate characterizations of some inherent but weak physical attributes become of critical importance, especially when the fundamental role of Kerr nonlinearity on capacity limits of fiber-optic communication systems is being extensively discussed [8]. However, the nonlinear coefficient of an ARF is expected to be 3-4 orders of magnitude smaller than standard single-mode fibers, resulting in a big challenge to perceive nonlinear phase shifts by self-phase-modulation induced spectral changes [9] or dual-frequency four-wave-mixing sidebands [10]. S. A. Mousavi et al. adopted spectrum measurements to study the nonlinear dynamic of picosecond pulse propagation in air-filled ARFs and reported a measured nonlinear refractive index (n_2) of atmospheric air of $\sim 6 \times 10^{-23} \text{ m}^2/\text{W}$ [11]. However, considering that Raman effects of Nitrogen play a key role in that experiment, the accuracy of this result (as well as its coincidence with Ref. [9]) is doubtful.

In this work, for precisely measuring the Kerr nonlinear coefficient of an ARF, a novel method of nonlinear phase shift estimation in the constellation diagram of high-order QAM signals is proposed and experimentally employed. Compared to traditional method of propagating femtosecond or picosecond laser pulses into a short-length ARF, our method circumvents the measurement inaccuracy caused by non-ideal beam launch, spectrum acquisition, and fiber length estimation. More importantly, only Kerr nonlinearity (with no Raman scattering) is accounted for. By using a real-time 400 Gb/s dual-polarized 64 quadrature amplitude modulation (DP-64QAM) optical module and a high-power erbium doped fiber amplifier (EDFA) with an output of 37.5 dBm, i.e. 5.6 W, we manage to measure the upper limit of $n_{2,\text{Kerr}}$ to be $2.20 \times 10^{-23} \text{ m}^2/\text{W}$, about 3 order magnitudes lower than n_2 in G.652.D. and about one-third of the result in Ref. [11].

2. Principle of nonlinear phase shift measurement

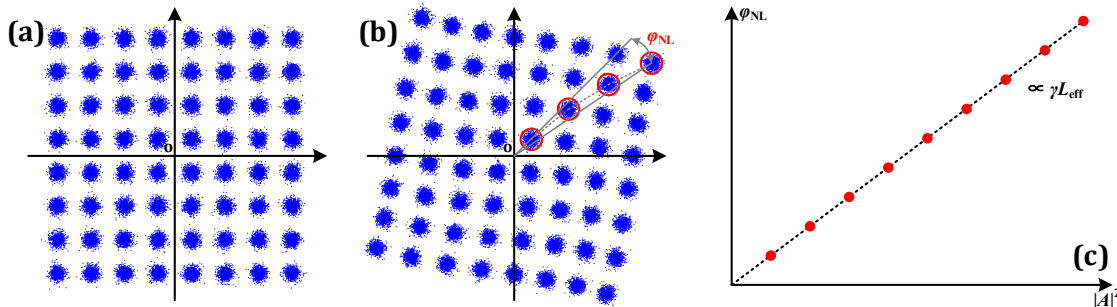


Fig. 1 Illustrative constellation diagrams of 64QAM signals (a) without and (b) with experiencing nonlinear phase shifts. (c) Schematic of linearly fitting nonlinear phase shifts with the variation of $|A|^2$.

The 3rd-order susceptibility $\chi^{(3)}$ induced Kerr nonlinearity gives rise to an additional phase shift after light propagation. The transmitted optical pulses at the end of a fiber can be written as

$$A(L, t) = A(0, t) \cdot e^{-\alpha L + j\varphi_{NL}}, \quad (1)$$

with the additional nonlinear phase shift $\varphi_{NL} = \gamma L_{eff} |A(0, t)|^2$ being proportional to the intensity of the signal. Here, A stands for the complex amplitude of the pulse, α is the attenuation coefficient, γ is the nonlinear coefficient, t is the time, and L ($L_{eff} = [1 - \exp(-\alpha L)]/\alpha$) is the (effective) fiber length. Taking 64QAM signal as an example [Fig. 1(a)], all the points inside the constellation diagram can be divided into ten groups according to their intensities (i.e., the square modules of A , or simply the square distances between these points and Point O). After propagation through a fiber, different nonlinear phases can be experienced by signal pulses of different intensities and give rise to a spiral rotation across the whole constellation diagram, as shown in Fig. 1(b). After signal demodulation, these additional phase shifts can be acquired at each constellation point by measuring the rotation angles. Accordingly, a linear fit of the nonlinear phase shifts and the distances between the constellation points and the original point (O) can be attained [Fig. 1(c)]. The slope of this fitting curve ($k = \gamma L_{eff}$) should be in proportion to the nonlinear coefficient (γ) of the tested fiber. And, on the basis of $\gamma = 2\pi n_2/(\lambda A_{eff})$, with λ the working wavelength and A_{eff} the effective mode area, the nonlinear refractive index (n_2) of the fiber medium can be derived as

$$n_2 = \frac{k\lambda A_{eff}}{2\pi L_{eff}} \quad (2)$$

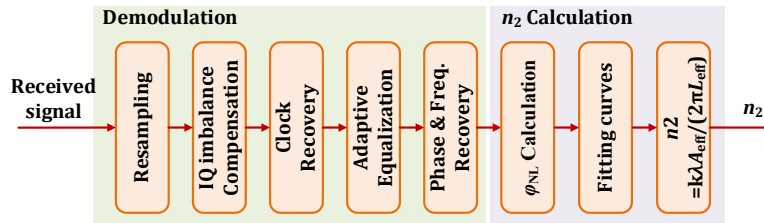


Fig. 2 DSP procedure for n_2 measurement.

The digital signal processing (DSP) for measurement is shown in Fig. 2. It should be noted that for high-order QAM signal, constellation points of different intensities are uniformly distributed in time. Consequently, the nonlinear phase shift measurements for different pulse intensities are also uniformly distributed in time. Therefore, in the DSP procedure, nonlinear phase shift will not be compensated in the stage of phase and frequency recovery, which provide solid foundation to our n_2 measurement. Compared to the previous pulse propagation measurement methods [9,11], the advantages of our method are twofold. Firstly, the introduction of high-order QAM transmission provides multiple measurable constellation points with different nonlinear phase shifts, therefore rendering a more accurate data fitting. Secondly, our coherent-detection-based measurement rules out all the nonlinear contributions from inelastic effects such as Raman scattering and Brillouin scattering. It is well known that both rotational and vibrational Raman frequency shifts are far out of band [11]. The nonlinear coefficient we measured only comes from Kerr effect.

3. Fiber fabrication and high-power data transmission experiment

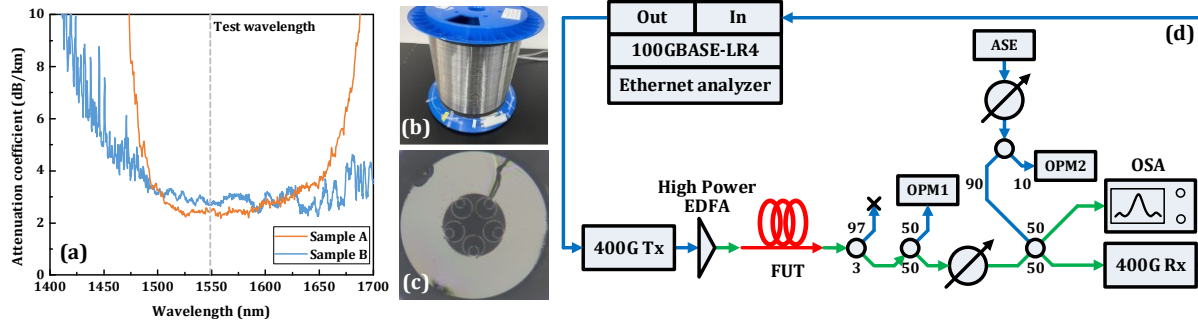


Fig. 3 (a) Cut-back measured loss spectra, (b) photograph, and (c) cross-section of the fabricated NNF-5 fibers. (d) Data transmission setup.

Two similar NNF-5 fibers (Samples A and B) are fabricated with the lengths of 466 m and 526 m, respectively. Fig. 3(a) shows their loss spectra measured by the cut-back method. Figs. 3(b) and 3(c) show the photograph and the cross-section of Sample B, whose effective mode area (A_{eff}) is measured to be $\sim 572 \mu\text{m}^2$ by a CCD camera at 1550 nm. Using home-made anti-reflection-coated interconnections [12] with typical insertion losses of 0.4 ~ 0.7 dB, these two NNF-5 fibers form a link with the total length of ~ 1 km and the total loss of 5.1 dB. The data transmission setup is shown in Fig. 3(d). A 400Gb/s DP-64QAM real-time optical module is used as the transmitter and receiver with the central wavelength set at 1548.515 nm. No nonlinearity compensation process is employed in the 400G module. A 100GBASE-LR4 module and an ethernet analyzer (VIAMI ONT 603) is used for error checking after transmission and forward error correction (FEC). The 400G signal is then boosted by a high-power EDFA (KEOPSSYS CEFA-C-

PB37), whose maximum output power is measured to be 37.8 dBm. Hence, thanks to the adoption of low-loss fiber interconnections [12], the actual power launched into our NANF-5 can be as large as 37 dBm (5 W). The noise figure of our high-power EDFA is < 6.5 dB, meaning that the penalty induced by EDFA is negligible. We also prepare 1-km G.652.D and 1-km G.654.E fibers for comparison. We measured the pre-FEC BER curves under different launch powers for all the three fibers, as shown in Fig. 4(a). It is seen that the constellation diagrams in Figs. 4(f) and 4(h) explicitly exhibit spiral rotations, indicating Kerr nonlinearity induced phase shifts. In contrast, for the NANF-5 link, only slight performance degradation in terms of BER is observed under 5-W launch power. We also measure the BTB case with about 5-m patch cord remained. Its pre-FEC BER curve overlaps precisely with the curve of 1-km NANF-5 link. After deduction of the OSNR penalty caused by the patch cord, we have not seen any more OSNR penalty attributed to the 1-km NANF-5 link even under 5-W launch power.

Although direct nonlinear phase shifts of our NANF-5 has not been observed, the above measurement still can provide an upper limitation to $n_{2,Kerr}$. The difference between the OSNR penalties of 1-km NANF-5 and 5-m patch cord is measured to be less than 0.01 dB due to our OSNR measurement resolution, while the OSNR penalty of 5-m patch cord is ~ 0.40 dB. In small nonlinear penalty region, the OSNR penalty can be approximated to be in proportion to the launch power (in linear scale). Exploiting the linear relationship of nonlinear phase shift and launch power, the Kerr nonlinearity of 1-km NANF-5 is over 40 times less than that of 5-m patch cord. The penalty of 5-m patch cord under 37-dBm launch power is roughly equivalent to the penalty of 1-km G.652.D under 14-dBm launch power. Taking into account all the parameters of fiber length, launch power, and A_{eff} , we estimate $n_{2,Kerr}$ of NANF-5 medium to be $< 2.20 \times 10^{-23}$ m²/W at 1550 nm, fitting well with the result of $n_{2,Kerr} = 2.3 \pm 0.3 \times 10^{-23}$ m²/W for N₂ in Ref. [9].

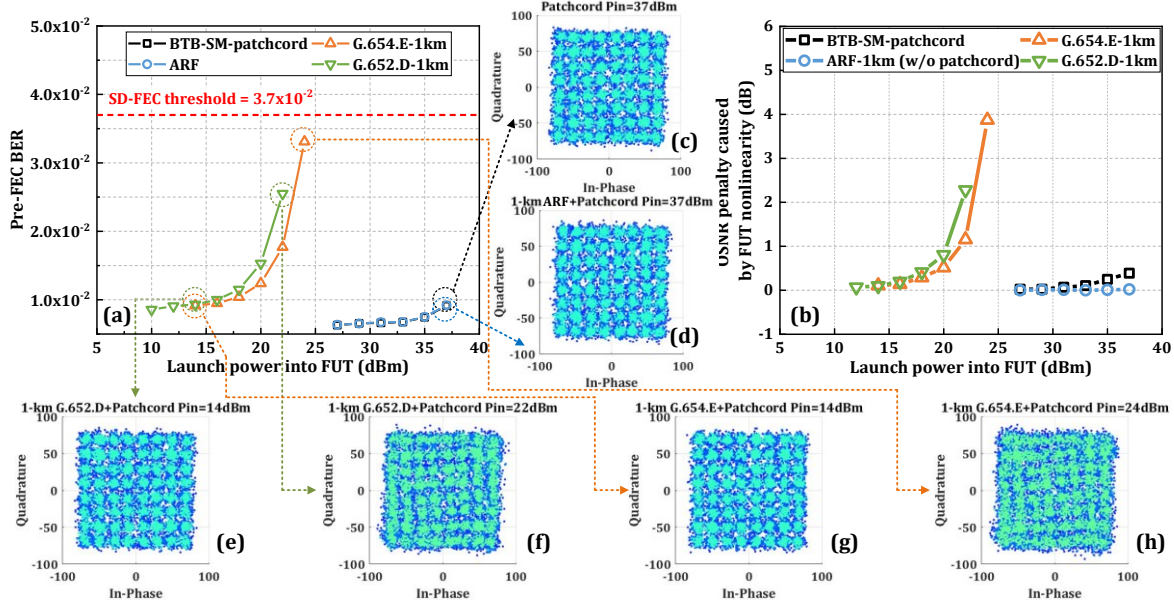


Fig. 4 (a) Measured pre-FEC BER and (b) derived OSNR penalties caused by fiber nonlinearity for BTB (black), 1-km NANF-5 + patch cord (blue), 1-km G.652.D + patch cord (green), and 1-km G.654.E + patch cord (orange). (c-h) Constellation diagrams retrieved at different circumstances.

4. Conclusions

In conclusion, we propose an accurate measurement technique for Kerr nonlinearity of ARF by estimation of nonlinear phase shift in high-order QAM transmission. By using a real-time 400Gb/s DP-64QAM, we give the upper limitation of the nonlinear refractive index of ARF medium ($n_{2,Kerr} < 2.20 \times 10^{-23}$ m²/W), which is 3 order magnitudes lower than G.652.D fiber and fits the spectrally measured $n_{2,Kerr} = 2.3 \pm 0.3 \times 10^{-23}$ m²/W of atmospheric N₂. This work was supported by National Natural Science Foundation of China (61827820, 62075083, 62105122, U21A20506); Fundamental Research Funds for the Central Universities (21620316); Basic and Applied Basic Research Foundation of Guangdong Province (2021A1515011646, 2021B1515020030).

5. References

- [1] S. F. Gao et al, *Nat. Commun.*, **9**: 2828, 2018.
- [2] T. D. Bradley et al, *ECOC2018*, **Th3F.2**, 2018.
- [3] H. Sakr et al, *Proc. OFC2021* **F3A.4**, 2021.
- [4] G. T. Jasion et al, *OFC2022*, **Th4C.7**, 2022.
- [5] A. Nespola et al, *OFC2021*, **F3B.5**, 2021.
- [6] H. Sakr et al, *J. Lightwave Technol.*, **38**(11), 159, 2020.
- [7] O. Alia et al, *ECOC2021*, **Th2G.4**, 2021.
- [8] R. J. Essiambre et al, *J. Lightwave Technol.*, **28**(4), 662, 2010.
- [9] E. T. J. Nibbering et al, *JOSAB*, **14**(3), 650, 1997.
- [10] A. Boskovic et al, *OL*, **21**(24), 1966, 1996.
- [11] S. A. Mousavi et al., *Opt. Express*, **26**(7), 8866, 2018.
- [12] Z. Zhang et al., *Opt. Express*, **30**(9), 15149, 2022.